Beyond TiO2: Cerium-Doped Zinc Oxide as a New Photocatalyst for the Photodegradation of Persistent Pollutants

Beyond TiO2: Cerium-Doped Zinc Oxide as a New Photocatalyst for the Photodegradation of Persistent Pollutants.

M. C. Paganini, D. Dalmasso, C. Gionco, V. Polliotto, L. Mantilleri, P. Calza*

Abstract: We prepared via hydrothermal synthesis zinc oxide samples doped with cerium. The samples were characterized via powder X Ray Diffraction measurements, Diffuse Reflectance UV Vis spectroscopy, Scanning Electron Microscopy and Transmission Electron Microscopy with EDX (Energy Dispersive X-Ray spectroscopy) analysis, and BET (Brunauer–Emmett–Teller) surface area analysis. XRD measurements reveal the formation of highly crystalline materials; wurtzite is the most important.

All materials were tested using phenol as model molecule and their performances were compared with TiO_2 P25. The material showing the best performance, namely Ce-doped ZnO, was then used to abate some emerging pollutants. We chose three iodinated X-ray contrast agent (ICM), iopromide, iopamidol and diatrizoate, known to be recalcitrant to traditional advanced oxidation processes. In the presence of TiO_2 P25, all ICM exhibited a slow degradation, with $t_{1/2}$ ranging from 30 min (iopamidol) to 120 min (diatrizoate) and several hours are required for their complete disappearance. The employment of Ce-doped ZnO leads to a sharp increase in their disappearance, with $t_{1/2}$ obtained within 15 min (iopamidol) or 25 min (diatrizoate) and the complete abatement is achieved within 2h.

Introduction

Metal oxides semiconductors such as TiO_2, ZnO, WO_3 etc. have been attempted for the photocatalytic degradation of a wide variety of environmental contaminants. Heterogeneous photocatalysis based on nano-structured TiO_2 has been extensively studied as an important destructive technology leading to the total mineralization of a wide range of organic dyes. In some cases, ZnO exhibits a better photocatalytic efficiency than TiO_2, but only few works reported that the photocatalytic activity of ZnO is better than Degussa P25 titania (P25), [1] which has been proved to be one of the most efficient photocatalysts, and widely used as a benchmark. However, both TiO_2 and ZnO are activated only under UV irradiation because of their large band gap (3.2 and 3.4 eV respectively), which greatly limits their application in environmental decontamination as solar spectra only contain 5% of UV. Therefore, it is crucial to explore efficient methods to extend their photocatalytic response from UV to visible region. Previous papers by some of us demonstrated that it is possible, through the dispersion of small amounts of cerium ions within the matrix of different oxides (namely zirconium dioxide or zinc oxide), to modify the photoactivity of the final material. Thereby, the modified oxide becomes photoactive in visible light and much more active in UV light. [2, 3] In the case of zinc oxide the cerium does not enter into the structure forming a solid solution due to the deep difference in dimensions of the two metal ions, but segregates as cerium oxide. The interaction between the interfaces of the two oxides is the reason of the increased photocatalytic activity. Doped zinc oxide is a promising candidate as a photocatalytic material since it demonstrates high photocatalytic efficiencies for the degradation of organic pollutants and can be a suitable alternative to TiO_2 thanks to its very similar band gap and to the different morphologies in which it can be prepared.[4, 5]. Indeed very recently, some papers have been published about Ce-doped ZnO nanostructures used for photocatalytic applications, but in that case the photoactivity was not compared with TiO_2 P25 due to the fact that it was still less efficient.[6].

In a previous paper [3] we prepared pure and doped ZnO with low cerium loading (1% molar) via hydrothermal process, a low temperature, green and simple process to obtain controlled nanostructures, starting from acetate precursor using different Cerium precursors. In the present paper, we prepared materials via the same hydrothermal method, but starting from a different zinc oxide precursor, namely zinc nitrate, that permits to obtain an increased photoactivity. We decided to mantain the low concentration of cerium (1% mol) for using this sample in comparison with the other material we already prepared [3]. The photocatalytic performance of these new materials was firstly tested on phenol and then to more refractory compounds, such as iodinated X ray contrast agents (ICM).

Prof. Maria Cristina Paganini, Dr. Daniele Dalmasso, Dr. Chiara Gionco, Dr. Valeria Polliotto, Dr. Lorenzo Mantilleri, Prof. Paola Calza*
Department of Chemistry
University of Turin
Via P. Giuria 5-10125 Torino-Italy
E-mail:paola.calza@unito.it

ICM, a class of medical diagnostic agents used for imaging blood vessels and organs, are among the most recalcitrant and highly persistent emerging pollutants[7]. Large quantitiesof ICM are administered to individual patients undergoing tests (>100 g dose^{-1}), and are generally excreted unmetabolized within 24 h[8]. Although often considered to be biochemically inert, some researches had shown that diatrizoate may have nephrotoxic effects in animals and humans [9].Only limited biodegradation of ICM was reported during biological wastewater treatment processes and biotransformation is very slow in soil/sediment–water incubations (e.g., $t_{1/2}$> 20 days) [10], resulting only in partial modifications to the sidechains of the core triiodinated aromatic ring structure; especially ionic ICM like diatrizoate had shown to be remarkably resistant to biotransformation [11].

Conventional drinking water treatment processes have shown as well a slight success in removing or transforming ICM [12]. Conversely, electrochemical process [13] and advanced treatment processes, i.e. UV/H_2O_2[14], UV/O_3 and O_3/H_2O_2 had shown some success in degrading ICM. Only few works explore the employment of the photocatalytic treatment with TiO_2 toward ICM; Doll and Frimmel[15] reported on the UV-TiO_2 degradation of nonionic ICM (iomeprol and iopromide), evidencing a limited mineralization. Sugihara et al. [16]studied the kinetics and mechanisms for TiO_2photocatalytic transformation of diatrizoate and structurally related compounds in both oxic and anoxic aqueous suspensions. In the present paper, we explore the possibility to treat ICM with new materials based on ZnO aimed to increase the degradation efficiency of ICM under photocatalytic treatment.

Results and Discussion

Materials characterization

XRD analysis

XRD patterns of the samples investigated in this work are shown in Figure 1. The peculiar peaks corresponding to the diffraction patterns of hexagonal wurtzite phase of ZnO are observed. The pattern of undoped ZnO corresponding to (1 0 0), (0 0 2), (1 0 1), (1 0 2), (1 1 0), (1 0 3), (2 0 0), (1 1 2) and (2 0 1) planes are in accordance with the wurtzite hexagonal phase of ZnO [18].

The introduction of Cerium does not bring any modifications in the crystal structure of ZnO, but the cerium introduced as dopant in the sample segregates as CeO_2 phase as it can be seen in Figure 1, bottom; in particular the peak related to the (1 1 1) plane is observed. Moreover, in both samples some peaks, of very low intensity, related to the $NaNO_3$ phase can also be identified, being a residual from the synthesis procedure.

On the XRD patterns a Rietveld refinement was performed using the MAUD software [17]. Table 1 lists the calculated relative abundance of the two oxides, lattice parameters and average crystals size. The lattice parameters of ZnO are not influenced by the introduction of Ce. The ZnO crystallites are large (between 150 and 300nm), while the CeO_2 crystallites, obtained as segregation phase, are significantly smaller (about 10 nm).

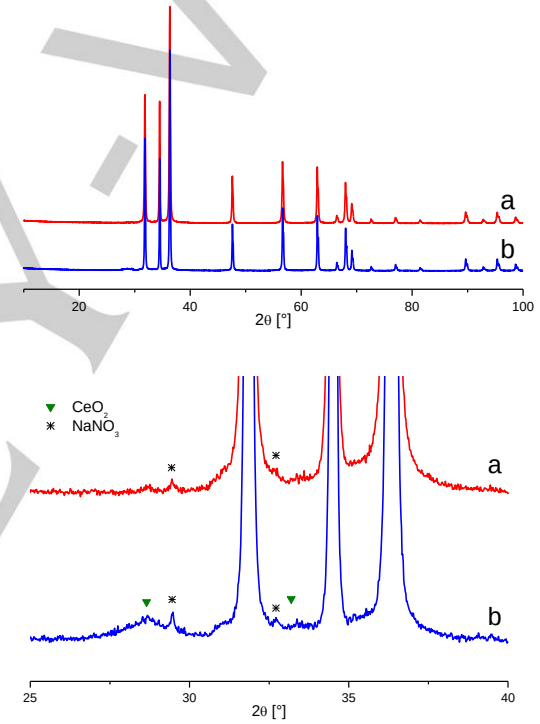

Figure 1. XRPD ptterns of ZnO (a) and Ce-ZnO (b). Top: full pattern. Bottom: Magnification of A.

Table 1. Cell parameters, weight and molar percentage and crystallite size obtained from Rietveld refinement of the XRD patterns of bare and doped ZnO. R_{wp} is the weighted residual error, *a* and *c* are lattice parameters, d is the average crystallite dimension.

Sample	Phase	R_{wp}	%mol	*a* [Å]	*c* [Å]	d [nm]
ZnO		9.15				
	ZnO		100%	3.252	5.210	160
Ce-ZnO		10.12				
	ZnO		99%	3.252	5.210	299
	CeO_2		1%	5.404		9

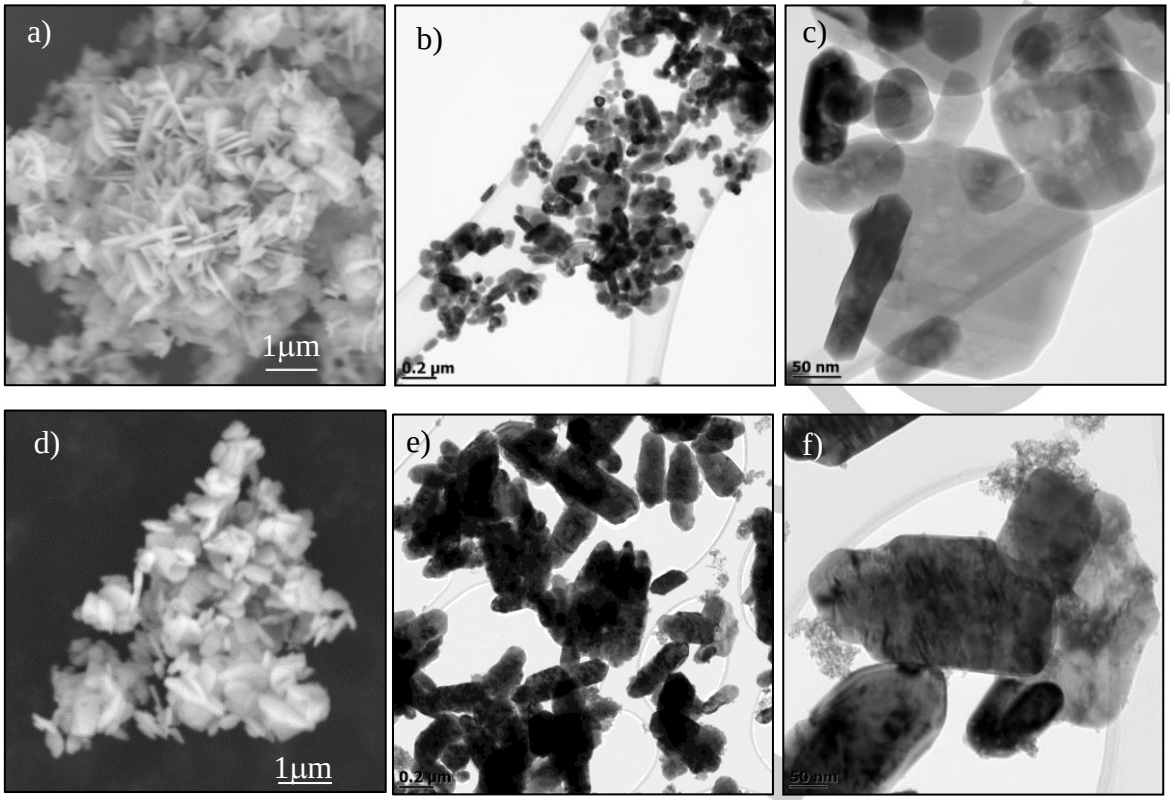

Figure 2. SEM (a, d) and TEM (b, c, e, f) images of ZnO (a, b, c) and Ce-ZnO (d, e, f).

Scanning Electron microscopy and Transmission Electron Microscopy analysis

Figure 2 depicts the surface morphology of pure ZnO (Fig. 2a, b, c) and Ce-ZnO (Fig. 2d, e, f) catalysts. The SEM images (Fig. 2 a and d) show the morphology of the particles: they look like platelets that form big aggregates. To be more specific, bare ZnO (Fig. 2a) exhibits clusters of platelets that form a sort of flower like hierarchical structure. On the other hand, the doped catalyst (Fig. 2d) with cerium chloride, revealed bigger flakes, which aggregate, leading to the formation of a cluster.

The TEM images (Fig. 2b, c, e, f), in which the particles are more dispersed than in SEM images, reveal that both catalysts present different morphologies and different dimension of particles: most of them look like large and thin platelets with different elongation according to the axes, other exhibit spherical or hexagonal plate-like shape. Ce-ZnO sample (Fig. 2 e and f) shows, for the wurtzite phase, crystals bigger than those of bare ZnO (Fig. 2 e and f), confirming the XRD results. Furthermore, the addition of Ce results in a complete segregation as little sferical particles of CeO_2, as one can deduce from the EDX map of Ce-ZnO sample, reported in Figure 3.

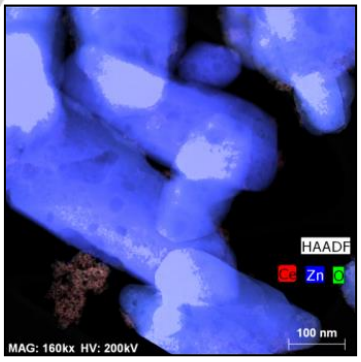

Figure 3. EDX atomic maps of Ce (red), Zn (blue) and O (green) for Ce-doped ZnO sample.

This map, indeed, shows that all Zn atoms form ZnO crystallites while the Ce atoms segregate in islands of CeO_2 joined to ZnO particles. On the contrary, the sample presents a good spatial dispersion of oxygen in both ZnO and CeO_2 crystals.

The chemical compositional analysis is very important to monitor the concentration of the dopant. The EDX analysis of the described samples (Table 2) shows that, as expected, only Zn and O are present in the non-doped sample of ZnO and that the total percentage of cerium in the doped sample is about 1.5%. The Ce/Zn molar ratio calculated from the atomic percentages is close to 1%, as expected from the nominal composition.

Table 2. Atomic percentage of elements obtained from EDX analysis

Sample	Elements	Atomic %	Ce/Zn ratio
ZnO	O	38.8	/
	Zn	61.2	
Ce-ZnO	O	35.7	0.94%
	Zn	62.8	
	Ce	1.5	

DRS UV-Vis analysis

We used the well-known TiO_2 P25 as reference sample for comparing the optical properties, surface area and, in particular, the photocatalytic efficiency. The optical spectra of the P25 sample and of bare and doped ZnO exhibit relatively small differences and confirm previous data reported in the literature [18]. Figure 4 shows the absorption spectra obtained for TiO_2 P25, ZnO and Ce-ZnO samples. As it can be seen the Ce doping of ZnO results in a very small increase in the overall absorption (see enlargement of Figure 4), towards the visible domain. The spectra are dominated by the valence band (VB) – conduction band (CB) transition occurring at about 400 nm (ca. 3 eV) for ZnO and Ce-ZnO, and at about 350 nm (ca. 3.5 eV) for P25.

Energy gap values have been calculated by linearization of the plot reporting $(\alpha h\nu)^{1/2}$ vs $h\nu$ typical of indirect band gap transitions for P25 and by linearization of the plot reporting $(\alpha h\nu)^2$ vs $h\nu$ typical of direct band gap transitions for ZnO and Ce-ZnO[19], results are reported in Table 3.

The calculated energy gap for the three samples are very as expected.

Table 3. Calculated energy gap (through the Tauc plot from DRS measures) and B.E.T. specific surface area (from nitrogen adsorption/desorption measures) of the samples.

Sample	E_g [eV]	S_{BET} [m^2/g]
P25	3.28	55
ZnO	3.26	<10
Ce-ZnO	3.27	<10

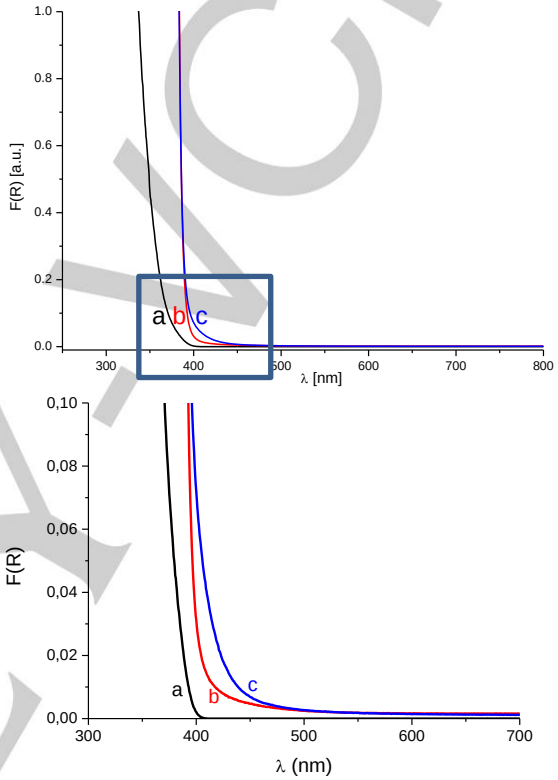

Figure 4. Absorption spectra of TiO_2 P25 (a), ZnO (b) and Ce-ZnO (c).

B.E.T. specific surface area

The specific surface area of the samples was measured applying the Brunauer–Emmett–Teller (B.E.T.) model on the N_2 adsorption measurement. The S_{BET} of the ZnO and Ce-ZnO samples results in a very low value, less than 10 m^2/g, compared to that of TiO_2 P25.

As it concerns the surface area we can just state that is low (less than 10 m^2/g) because of instrumental limits (N_2 adsorption is not fully reliable for systems having such a low area). Nevertheless such a low value is quite in agreement with the large values (> 150 nm) found with the XRD analysis.

The photocatalytic effect (see next paragraph) observed for the doped systems is due to the tiny shoulder indicating the presence of intra-band gap states and not to a real shift of the

band gap itself.[4] We think that these intra-band gap states are the responsible for the photocatalytic activity of the doped samples.

Photocatalytic performances

Degradation of phenol

Preliminary, we tested the behavior of bare and doped ZnO under UV-A irradiation in the photo-degradation of phenol, frequently used as probe molecule; for comparison purpose, P25 was employed as well. Direct photolysis and adsorption process in the dark are negligible. In a previous work [3], we explored the role of different dopant amounts and salt precursors on the catalyst efficiency and we concluded that the optimal dopant amount is fixed to 1%, while the best precursor salt was $CeCl_3$, due to favorable cerium oxidation state. Therefore, we produced our materials using these conditions but starting from two different zinc oxide precursors, namely zinc nitrate (ZnO) and zinc acetate (ZnOa).

Figure 5 shows the disappearance profiles for phenol over time in the presence of the synthetized materials and commercial TiO_2 P25. Interestingly, while the disappearance of the two molecules similarly occurred with both bare ZnO or commercial TiO_2 P25, the use of Cerium doped ZnO induced a sharp increase in the degradation of phenol. Doped zinc oxide prepared starting from nitrate salt (named ZnO-Ce) exhibits a higher activity than that synthetized via acetate precursor (named ZnOa-Ce). A possible explanation may lie in their different ability to produce a homogenous dispersion during the synthesis. In the presence of ZnO-Ce, phenol (P) is completely abated within 10 min of irradiation, while with ZnOa-Ce 30 min are required and even 60 min with P25. The early formed transformation products from phenol degradation are known to be catechol (Cat) and hydroquinone (HQ) [20] whose evolution profiles obtained using Ce-ZnO and TiO_2 are reported in the Figure 5 (bottom). When employing Ce-ZnO, HQ and Cat achieved the maxima concentration in few min and then they are easily degraded within 20 min of irradiation, so assessing that all aromatic compounds are completely abated. Conversely, with P25 their kinetic evolution are slowed down and up to 90 min are required. The performance of Ce-ZnO was also evaluated toward high phenol concentrations, aimed to test if this material is also suitable for the treatment of water with high content of organic pollutants. The photocatalytic degradation can be ascribed to a pseudo-first order kinetic model, so that the disappearance initial rate can be calculated by using mono-exponential decay, as described by the following equation:

$$C = C_0 e^{-kt}$$

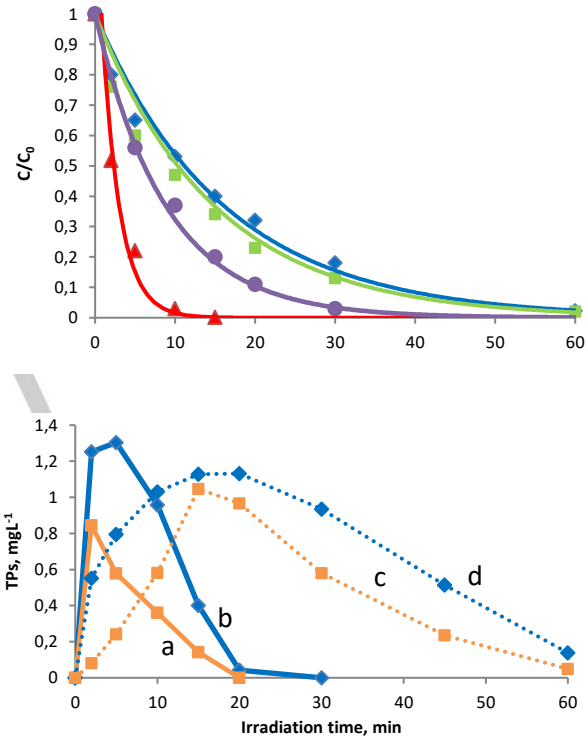

Figure 5. Phenol (10 mg/l) de gradation in the presence 1 g/l of bare ZnO (■) doped Ce-ZnO (▲),doped ZnOa-Ce (●) and P25 (♦) (top); (bottom) Transformation products formed following phenol degradation on Ce-ZnO and P25; (a) Cat Ce-ZnO, (b) HQ Ce-ZnO, (c) Cat P25, (d) HQ P25.

where C corresponds to pollutant concentration, k is the pseudo-first order kinetic constant, t is the reaction time and C_0 is pollutant concentration for t=0; the calculated pseudo-first order rate constants as a function of phenol concentration, as well as the half-lives ($t_{1/2}$), are plotted in Figure 6. Interestingly, when using Ce-ZnO phenol half-life time is reached within few minutes also when treating aqueous dispersion with high phenol content (i.e starting from 100 mg/L of phenol, 50% is degraded in 25 min), while with P25 half-life time increased up to 120 min.

By analyzing the initial rate in the different conditions, with P25 the rate level off for 60 mg/l of phenol, while with Ce-ZnO rate continues increasing up to 100 mg/L, so underlining that the photoactivity of doped material remains still high also when treating concentrated aqueous solution of phenol, thus opening the door to its exploitation in the treatment of samples with high content of organic matter.

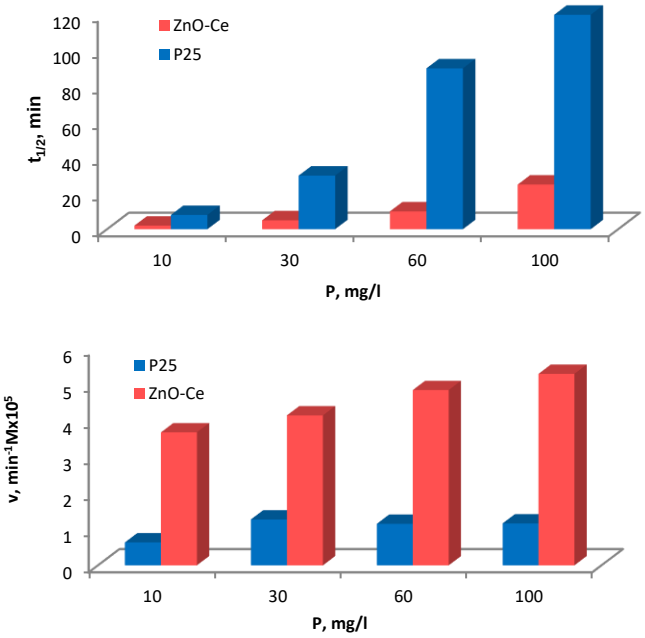

Figure 6. Phenol half-lives time (top) and rate (bottom) as a function of phenol (P) concentration in the presence of (a) Ce-ZnO and, for comparison, (c) P25 (1 g/l).

Degradation of X-ray contrast agents

The performance of ZnO and Ce-ZnO was also tested toward the photodegradation of some persistent iodinated X-ray contrast agents, namely iopamidol, iopromide and diatrizoate, three emerging contaminants known to be scarcely abated in the wastewater treatment plant [12]. The overall degradation curves for ICM are plotted in Figure 7, while the calculated initial rate constants are collected in Figure 8. Direct photolysis was assessed as blank experiment for all tested drug and, in all cases, was negligible. The employment of Ce-ZnO induced a strong increase in the degradation rate for all drugs. Considering iopamidol, its rate is 4 times higher when employing Ce-ZnO; half-life was shorten from 30 min (P25) to 2 min (Ce-ZnO) and the complete drug disappearance was achieved in only 30 min, while with P25 up to 4h are required.

A similar trend was observed with iopromide and diatrizoate, with a rate 3 times higher in the presence of Ce-ZnO and $t_{1/2}$ reduced from 40 (P25) to 15 min (Ce-ZnO) and from 2 h to 30 min, respectively; iopromide complete degradation was achieved within 2 h (Ce-ZnO) rather than 5 h (P25), while for diatrizoate degradation time passes from 16 h (P25) to 3h (Ce-ZnO).

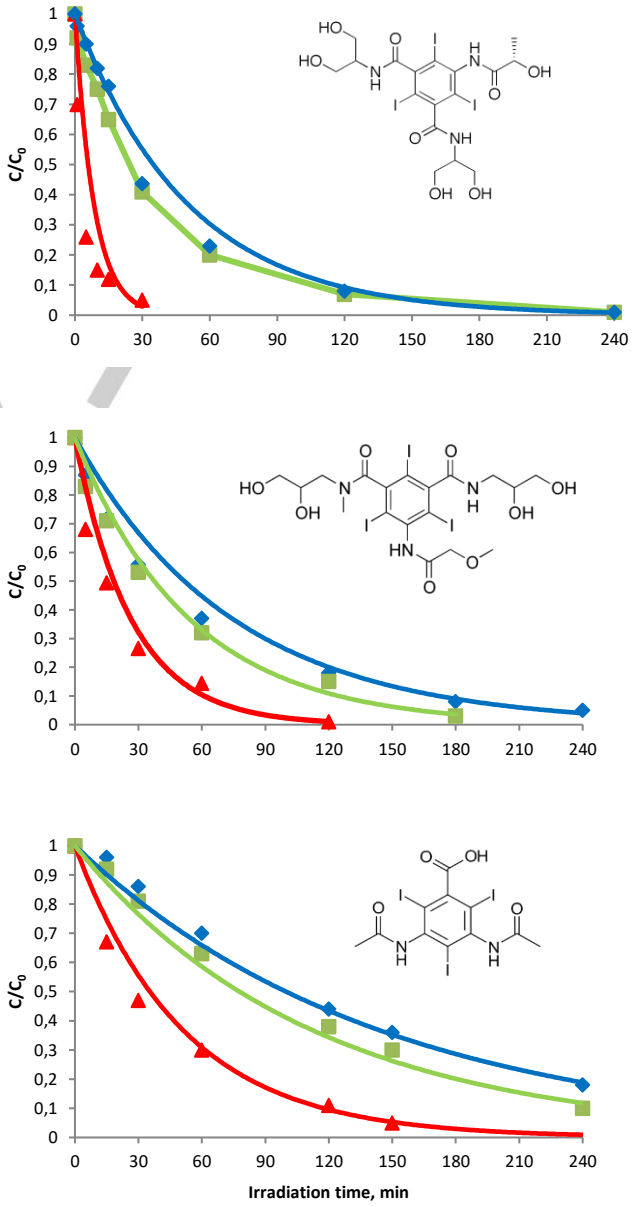

Figure 7. Iopamidol (top), iopromide (middle) and diatrizoate (bottom) (10 mg/l) degradation in the presence of bare ZnO (■) Ce-ZnO (▲) or (♦) P25 (1 g/l).

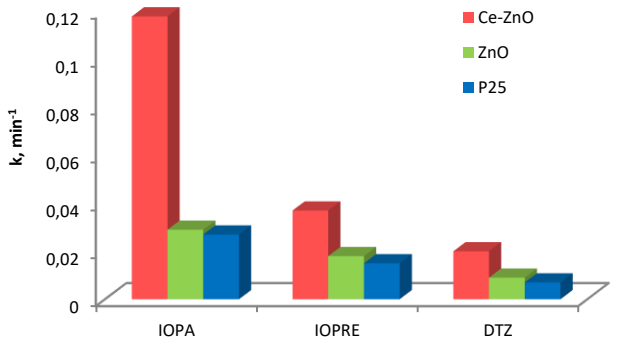

Figure 8. ICM constant rate in the presence of ZnO, Ce-ZnO and P25 (1 g/l).

We interpreted the higher photoactivity of the Ce-ZnO respect to the bare ZnO or to P25 in term of the role of intra band gap states generated in the doped material and in the interaction at the interfaces generated between ZnO crystallites with small amount of CeO_2 formed. Cerium, as most of the lanthanide, is stable in both the oxidation number +3 and +4 being the electronic configuration respectively $4f^1\ 6s^0$ and $4f^0\ 6s^0$, with the f orbitals close in energy to the other orbitals. F orbitals are mostly localized and less expanded respect to the d orbitals. These empty states (in the case of Ce^{4+}) act as a sort of link between the valence band and the conduction band of the oxide allowing low-energy photons to excite electrons from one band to the other. The mechanism, a sort of double jump photoexcitation, is analogous to that recently described by some of us to interpret the photocatalytic activity of N doped TiO_2 in visible light.[21] These factors, empty states as mid gap levels and junctions at the interfaces of different matrices, seem to be essential to ensure a certain efficiency to the two-photons excitation mechanism.

Conclusions

In this work we synthesized via hydrothermal process cerium doped zinc oxides. We used $CeCl_3$ as cerium precursor for the doping and the specific percentage of 1% molar of dopant has been selected as the most interesting according to the photocatalytic results obtained. The photocatalytic activity of the synthesized materials has been compared with the undoped material (bare ZnO) and with the benchmark TiO_2 P25 in the photodegradation of phenol used as probe molecule, at different concentrations. The obtained results of this preliminary screening were very encouraging. The synthesized material has been then tested also in the photodegradation of X-ray contrast agents, namely iopamidol, iopromide and diatrizoate, emerging contaminants known to be scarcely abated in the wastewater treatment plants. Also in this case the achievement of the complete drug disappearance in only 30 min was a great success especially if compared with the results present in the literature. ZnO doped with cerium chloride could represent an efficient candidate in the family of solar light photocatalysts.

Supporting Information Summary paragraph

In this paragraph the experimental section will be provided

Acknowledgements

We acknowledge support from a Marie Curie International Research Staff Exchange Scheme Fellowship (PHOTOMAT, proposalno. 318899) within the 7th European Community Framework Programme, project MAT4TREAT within the European Union's Horizon 2020 research and innovation programme under the Marie Skłodowska-Curie grant agreement No 645551 and the project funded by MIUR, in the frame of the collaborative international consortium WATERJPI2013-MOTREM of the Water Challenges for a Changing World Joint Programming Initiative (WaterJPI) Pilot Call and the Local Funding of the University of Torino call_2014_L2_126. P.C and MC P. also acknowledge the Alfatest Strumentazione Scientifica srl for providing SEM pictures and Prof. Z. Sojka (Jagellonian University of Cracow) for the TEM images.

Keywords: iodinated X-ray contrast agents, zinc oxide, phenol, photocatalysis, cerium-doped

[1] F. Lu, W. Cai, Y. Zhang, *Adv. Funct. Mater.* **2008**, *18*, 1047-1056; S. Sakthivel, B. Neppolian, M. V. Shankar, B. Arabindoo, M. Palanichamy, V. Murugesan, *Sol. Energy Mater. Sol. Cells* **2003**, *77*, 65-82.

[2] C. Gionco, M. C. Paganini, M. Chiesa, S. Maurelli, S. Livraghi, E. Giamello, *Appl. Catal. A-Gen.* **2015**, *504*, 338-343.

[3] P. Calza, C. Gionco, M. Giletta, M. Kalaboka, V. A. Sakkas, T. Albanis, M. C. Paganini, *J. Hazard. Mater.* **2016**, In press.

[4] N. C. S. Selvam, J. J. Vijaya, L. J. Kennedy, *J. Nanosci. Nanotechnol.* **2014**, *14*, 2317-2324.

[5] K. G. Kanade, B. B. Kale, J. O. Baeg, S. M. Lee, C. W. Lee, S. J. Moon, H. J. Chang, *Mater. Chem. Phys.* **2007**, *102*, 98-104; C.

Gionco, M. C. Paganini, E. Giamello, R. Burgess, C. Di Valentin, G. Pacchioni, *J. Phys. Chem. Lett.* **2014**, *5*, 447-451.
[6] M. Aslam, M. T. Qamar, M. T. Soomro, I. M. I. Ismail, N. Salah, T. Almeelbi, M. A. Gondal, A. Hameed, *Appl. Catal., B* **2016**, *180*, 391-402; J.-C. Sin, S.-M. Lam, K.-T. Lee, A. R. Mohamed, *J. Mol. Catal. A: Chem.* **2015**, *409*, 1-10.
[7] J. E. Drewes, P. Fox, M. Jekel, *J. Environ. Sci. Health., Part A* **2001**, *36*, 1633-1645; W. Seitz, J. Q. Jiang, W. H. Weber, B. J. Lloyd, M. Maier, D. Maier, *Environ. Chem.* **2006**, *3*, 35-39; R. L. Oulton, T. Kohn, D. M. Cwiertny, *J. Environ. Monit.* **2010**, *12*, 1956-1978; T. A. Ternes, R. Hirsch, *Environ. Sci. Technol.* **2000**, *34*, 2741-2748.
[8] T. Reemtsma, M. Jekel, *Organic Pollutants in the Water Cycle: Properties, Occurrence, Analysis and Environmental Relevance of Polar Compounds*, **2006**.
[9] M. E. Gale, A. H. Robbins, R. J. Hamburger, W. C. Widrich, *AJR Am J Roentgenol* **1984**, *142*, 333-335; H. D. Humes, D. A. Hunt, M. D. White, *Am. J. Physiol.* **1987**, *252*, F246-F255.
[10] J. L. Kormos, M. Schulz, H.-P. E. Kohler, T. A. Ternes, *Environ. Sci. Technol.* **2010**, *44*, 4998-5007; A. L. Batt, S. Kim, D. S. Aga, *Environ. Sci. Technol.* **2006**, *40*, 7367-7373.
[11] W. Kalsch, *Sci. Total Environ.* **1999**, *225*, 143-153; A. Haiss, K. Kummerer, *Chemosphere* **2006**, *62*, 294-302.
[12] P. Westerhoff, Y. Yoon, S. Snyder, E. Wert, *Environ. Sci. Technol.* **2005**, *39*, 6649-6663.
[13] G. Del Moro, C. Pastore, C. Di Iaconi, G. Mascolo, *Sci. Total Environ.* **2015**, *506*, 631-643.
[14] R. R. Singh, Y. Lester, K. G. Linden, N. G. Love, G. E. Atilla-Gokcumen, D. S. Aga, *Environ. Sci. Technol.* **2015**, *49*, 2983-2990.
[15] T. E. Doll, F. H. Frimmel, *Catal. Today* **2005**, *101*, 195-202; T. E. Doll, F. H. Frimmel, *Water Res.* **2005**, *39*, 847-854; T. E. Doll, F. H. Frimmel, *Water Res.* **2004**, *38*, 955-964.
[16] M. N. Sugihara, D. Moeller, T. Paul, T. J. Strathmann, *Appl. Catal., B* **2013**, *129*, 114-122; S. Carbonaro, M. N. Sugihara, T. J. Strathmann, *Appl. Catal., B* **2013**, *129*, 1-12.
[17] L. Lutterotti, *Nucl. Instrum. Methods Phys. Res., Sect. B* **2010**, *268*, 334-340.
[18] M. Rezaei, A. Habibi-Yangjeh, *Mater. Lett.* **2013**, *110*, 53-56.
[19] G. Martra, E. Gianotti, S. Coluccia, in *Metal Oxide Catalysis*, Wiley-VCH Verlag GmbH & Co. KGaA, **2009**, pp. 51-94.
[20] C. Minero, G. Mariella, V. Maurino, E. Pelizzetti, *Langmuir* **2000**, *16*, 2632-2641; Z. Guo, R. Ma, G. Li, *Chem. Eng. J.* **2006**, *119*, 55-59.
[21] G. Barolo, S. Livraghi, M. Chiesa, M. C. Paganini, E. Giamello, *J. Phys. Chem. C* **2012**, *116*, 20887-20894.

Entry for the Table of Contents (Please choose one layout)

Layout 1:

FULL PAPER

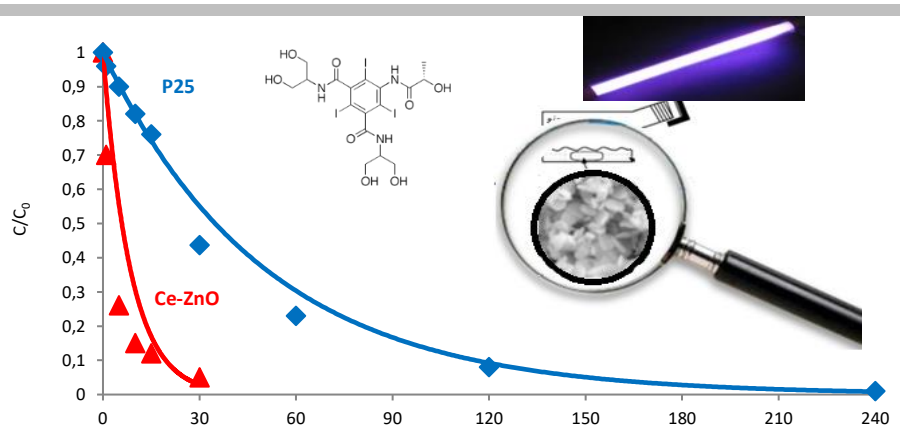

*M. C. Paganini, D. Dalmasso, C. Gionco, V. Polliotto, L. Mantilleri, P. Calza**

Page No. – Page No.

Title: Beyond TiO_2: Cerium-Doped Zinc Oxide as a New Photocatalyst for the Photodegradation of Persistent

In this paper aphotocatlyst of new generation photacatalyst based on ce doped Zinc Oxide has been synthesized, characterized and tested in the abatement of phenol, Iopamidol, iopromide and diatrizoate pollutants. It is more efficient than the most known titania P25.

Layout 2:

FULL PAPER

((Insert TOC Graphic here; max. width: 11.5 cm; max. height: 2.5 cm))

*Author(s), Corresponding Author(s)**

Page No. – Page No.

Title

Text for Table of Contents